

Article

# Assessment of Water Quality in a Coastal Region of Sea Dike Construction in Korea and the Impact of Low Dissolved Oxygen Concentrations on pH Changes

Yong-Woo Lee <sup>1</sup>, Yong Hwa Oh <sup>2</sup>, Sang Heon Lee <sup>3</sup> , Dohyun Kim <sup>1</sup> and DongJoo Joung <sup>3,\*</sup>

<sup>1</sup> Marine Environment Monitoring Department, Korea Marine Environment Management Corporation, Busan 49111, Republic of Korea; wbluesea@koem.or.kr (Y.-W.L.); dhkim@koem.or.kr (D.K.)

<sup>2</sup> Department of Convergence Study on the Ocean Science and Technology, Korea Maritime and Ocean University, Busan 49112, Republic of Korea; yhoh@kmou.ac.kr

<sup>3</sup> Department of Oceanography, Pusan National University, Busan 46241, Republic of Korea; sanglee@pusan.ac.kr

\* Correspondence: dongjoo.joung@pusan.ac.kr

**Abstract:** To investigate the factors affecting water quality in coastal regions with sea dike constructions, surface water outside a sea dike was monitored for six years from 2015 to 2020 in the Saemangeum region of Korea. Statistical analyses of the six years of high-frequency measurements revealed that the water quality in this system was predominantly governed by natural processes followed by pollutant inputs as the secondary influencing factor. Severe dissolved oxygen (DO) depletion was observed in the surface waters during warm periods, probably owing to the advection of DO-depleted water from elsewhere to the surface layer. Based on the apparent oxygen utilization (AOU)–pH relationship ( $r = 0.52$ ,  $n = 1837$ ), the maximum AOU (180  $\mu\text{M}$ ) led to a pH decrease from 8.04 to 7.50, which was considerably lower than the estimated value of 7.72. This extra pH drop was probably due to a reduction in the buffering capacity associated with increased  $\text{CO}_2$  in the water column originating from the atmosphere and in situ production, as well as local water column redox reactions associated with benthic inputs of reduced chemical species. Overall, persistent DO depletion with ongoing eutrophication/hypoxia could accelerate ocean acidification in Korean coastal waters, which could be more acute in coastal regions with artificial coastal constructions.

**Keywords:** water quality; sea dike; hypoxia; pH; apparent oxygen utilization; Republic of Korea



**Citation:** Lee, Y.-W.; Oh, Y.H.; Lee, S.H.; Kim, D.; Joung, D. Assessment of Water Quality in a Coastal Region of Sea Dike Construction in Korea and the Impact of Low Dissolved Oxygen Concentrations on pH Changes. *J. Mar. Sci. Eng.* **2023**, *11*, 1247. <https://doi.org/10.3390/jmse11061247>

Received: 16 May 2023

Revised: 10 June 2023

Accepted: 12 June 2023

Published: 19 June 2023



**Copyright:** © 2023 by the authors. Licensee MDPI, Basel, Switzerland. This article is an open access article distributed under the terms and conditions of the Creative Commons Attribution (CC BY) license (<https://creativecommons.org/licenses/by/4.0/>).

## 1. Introduction

Water quality is a critical issue in coastal regions, where increasing populations create serious environmental problems such as coastal water pollution, disruption of marine ecosystems, and coastal erosion attributed to artificial construction [1]. These problems could result in reductions in fisheries and restriction of leisure activities, affecting the livelihood of people living along the coastal regions. Coastal water quality is critical for all marine plants and animals. In particular, primary production is affected by nutrient conditions and water transparency that controls light radiation [2]. Due to carbon fixation by phytoplankton, coastal water quality can also be viewed as an important factor in the global climate crisis [3]. Marine water quality also affects fish and mammals not only through the trophic disturbances associated with the primary producer but also through exposure to toxicants (e.g., metals) originating from nearby land and cities [4]. Therefore, developing qualitative and quantitative assessment tools is necessary to address the situation and predict changes in coastal environments.

Artificial construction in coastal regions, such as massive harbors and land reclamation, affects water quality and, subsequently, the coastal ecosystem. Typically, the effects of coastal construction on a marine ecosystem include weakened tidal currents, tidal prisms,

bay–shelf exchange, sediment relocation, and coastal erosion [5]). Recently, Perkins et al. [6] reviewed the impacts of coastal construction on marine ecosystems and revealed that artificial construction strongly affects the community structure, inter-habitat linkages and ecosystems, and leads to habitat loss, all of which directly impact human society (e.g., enhancement of fisheries, carbon sequestration). Moreover, intertidal habitats harbor various environments that span abiotic gradients, such as immersion and emersion tidal cycles, sediment characteristics and dynamics, wave exposure, current velocity, salinity, pH, temperature, and oxygen [7]. Therefore, coastal structures in intertidal habitats, in addition to habitat loss from the footprint of a structure, also impact the abiotic conditions and lead to subsequent cascading biological effects [6]. However, studies on water quality associated with artificial construction are still scarce, particularly for waters outside the sea dike.

Coastal construction induces a change in the current and mixing patterns of water masses [8]; thus, it has the potential to impact hypoxic water development (dissolved oxygen concentration (DO) < 2 mg/L). This low oxygen condition in coastal waters is increasing and is perhaps the most prominent problem caused by coastal eutrophication, which leads to changes in the water chemistry, such as increases in CO<sub>2</sub> concentrations and reductions in pH [9]. Coastal construction can either reduce or intensify hypoxic water development. Karim et al. [8] investigated the evolution of bottom water hypoxia in a bay using a complex model and suggested that land reclamation could cause the upwelling of hypoxic bottom waters in summer due to the current changes associated with seawall construction, thereby replacing hypoxic bottom water with DO-rich surface waters. In contrast, using a numerical model, Yamaguchi and Hayama [10] suggested that dike construction caused bottom water hypoxia both inside and outside the dike and in wide areas of the Ariake Sea in Japan because the dike reduces the tidal current and estuarine circulation, which intensifies water column stratification, thus causing bottom water hypoxia. Therefore, the link between changes in water chemistry and artificial coastal construction is not completely understood.

Bottom water hypoxia indicates that the sediments and overlying water enter reducing conditions, which increase water column remineralization and sedimentary fluxes of chemical constituents to overlying waters, potentially negatively affecting the marine biota. For example, in waters from the Louisiana Shelf in the northern Gulf of Mexico, Joung and Shiller [11] observed 2–3 orders of magnitude higher concentrations of dissolved Fe and Mn in hypoxic waters than in non-hypoxic waters. In the same regions, Cai et al. [9] found a decrease in water pH during the bottom water hypoxia season. Several coastal seas in Korea are also experiencing low DO conditions in bottom waters [12,13], and this bottom water hypoxia is likely to occur in many bays along the Korean coast due to the number of fish farms that release nutrients and organic matter [14]. Moreover, with ongoing global warming, coastal eutrophication and zones of bottom water hypoxia are expected to grow in size and duration across the globe [15,16], making changes in water chemistry a global phenomenon in the near future. Therefore, water quality management is critical from the enviro-climatological perspective.

In this study, we examined coastal water quality in the Saemangeum land reclamation area in southwestern Korea, which was completed in 2006 with the construction of a 33 km long sea dike. During and after this artificial construction, some adverse effects were observed in the artificial lake created by the sea dike, such as elevated chemical pollutants and nutrients [17] and related eutrophication and low oxygen levels in bottom water [18]. However, most previous studies were conducted within the artificial lake (inside the sea dike) and in rivers feeding into the lake (e.g., [17,19–21]), not outside of the sea dike, despite the potential negative effects of artificial construction on water quality. The primary aims of this study are to examine the water quality outside the sea dike and to discern the potential alterations in water chemistry that can be attributed to the artificial construction. In this study, we investigated water quality outside the sea dike using high-frequency measurements of nine variables for six years from 2015 to 2020. Through statistical analysis,

we determined the primary factors affecting water quality and further discuss surface water DO depletion and its impact on water chemistry. Our findings can provide crucial information for water quality and ecosystem management outside sea dikes.

## 2. Methods and Materials

### 2.1. Site Description

Surface seawater was monitored at a site off the Saemagum sea dike located in the mid-west of South Korea (Figure 1). The construction of this artificial dike was initiated as part of the Saemangeum Reclamation Project, which involved reclaiming 283 km<sup>2</sup> of wetlands and estuaries by constructing a 33 km long sea dike. When the seawall was completed in 2006, it enclosed a reservoir of approximately 120 km<sup>2</sup>, with a water-securing capacity of approximately 535 million tons of freshwater [22]. This Saemangeum artificial lake receives terrigenous effluents mainly from the Mangyeong and Dongjin Rivers, and their annual freshwater discharges are  $1100 \times 10^6$  and  $700 \times 10^6$  m<sup>3</sup>/year, respectively [19]. The water level of the Saemangeum artificial lake is maintained at 1.6 m below sea level [23], and thus, water exchange between the coastal waters and the artificial lake is restricted, occurring only episodically when it is necessary to control the water level and quality, such as during heavy precipitation in the watershed or during drought. Before construction, the tidal range in the study area was up to 6 m; after construction, it is less than 1 m, even when the sluice gates are fully open [24,25]. The mean monthly air temperatures range from  $-0.4$  °C (January) to  $25.7$  °C (August), and the mean annual precipitation is 1204 mm; precipitation mainly occurs during summer (June to September), which accounts for more than 65% of the total annual precipitation [26].

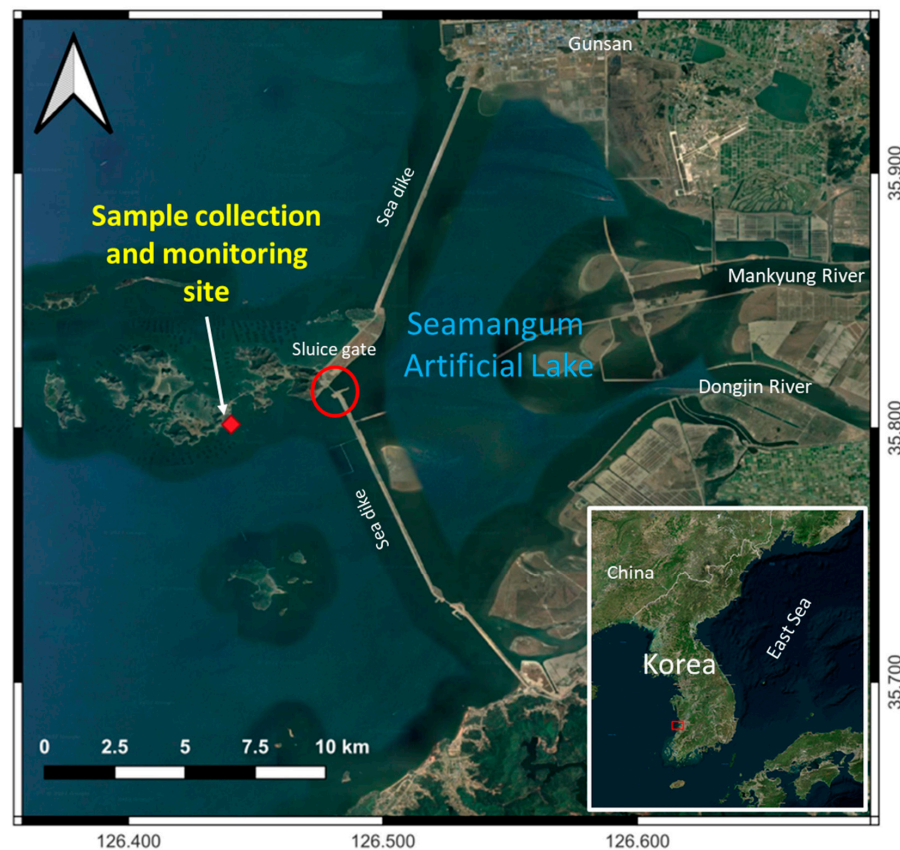


**Figure 1.** Map of the sample collection site. The red diamond indicates the facilities where all monitoring sensors were installed. Water was collected at about 50 m from the measurement site. In the inset figure, the red rectangle indicates the study area. The red circle indicates the location of the sluice gate.

## 2.2. Sample Measurements

The data used in this study were collected through the National Marine Environmental Measuring Network Program (<https://www.koem.or.kr>, accessed 5 June 2022). The surface water was monitored for temperature, salinity, pH, dissolved oxygen (DO), turbidity (nephelometric turbidity unit; NTU), chlorophyll *a* (Chl *a*), total nitrogen (TN), total phosphorus (TP), and chemical oxygen demand (COD). Surface water was continuously pumped to a measurement facility equipped with multiple sensors and analyzers. Salinity, temperature, pH, DO, and Chl *a* were collected using monitoring sensors (YSI6600EDS YSI, Yellow Springs, OH, USA), and COD, TN, and TP were determined by online auto-analyzers (Robochem S Centennial Technology Corporation, Ansan, Republic of Korea). The accuracies of the temperature, salinity, pH, DO, turbidity, and Chl *a* measurements were  $\pm 0.15$  °C,  $\pm 0.01$  unit,  $0.2 \text{ mgL}^{-1}$ ,  $\pm 2\%$ , and  $0.1 \text{ }\mu\text{gL}^{-1}$ , respectively. The precision of the TN, TP, and COD measurements was 3%. The measurements were conducted during water flow at a rate of  $\sim 50 \text{ L/min}$  to minimize the artifacts that could originate from water storage or delayed measurement. Among the nine variables, temperature, salinity, pH, DO, turbidity, and Chl *a* were measured every 5 min, and the others were measured once per hour. These sensors and analyzers were maintained once a week and occasionally upon malfunction. The measurement facility was located approximately 50 m from the sample collection site, which was approximately 3 km from the sluice gate (Figure 1). The sample collection site had a total water depth of 3 m, and water was collected at a depth of  $\sim 1 \text{ m}$  from the surface.

## 2.3. Statistical Analysis

The high-frequency (every 5–60 min) measurements from 2015 to 2020 provided more than 35,000 data points for each variable (Supplementary Table S1). Because the variables measured every 5 min did not change significantly within 1 h (Supplementary Figure S1), we collected one datum per hour. After extraction, the values were averaged to a day scale for further statistical analysis.

Multivariate statistical analyses, such as principal component analysis (PCA) and cluster analysis (CA), were employed to identify the primary factors responsible for temporal variations in water quality. A detailed description of the PCA application can be found elsewhere (e.g., [27]). Briefly, a multi-variation correlation matrix that presents the inter-connection correlation among all variables and the degree of significance of the respective correlations was generated [28]. Based on the multi-variation correlation significance, the numbers of variables were grouped, creating a new, uncorrelated variable that has a linear combination with the original variables [27]. Thus, the original variable dimension could be reduced to fewer summarized components. CA is commonly used to classify groups of parameters that behave similarly and helps identify the possible factors or sources influencing water quality [29,30]. All statistical analyses were performed using IBM SPSS version 26 (IBM, Armonk, NY, USA).

## 3. Results and Discussion

### 3.1. General Distribution

Hourly detailed graphs (original dataset) are shown in the Supplementary Information (Supplementary Figures S1–S6). For data handling and interpretation, hourly data were averaged into daily and monthly data. Thus, we reduced over 35,000 data points to approximately 1700 and 71 data points for the daily and monthly scales, respectively (Figures 2–4). In brief, during the study period from 2015 to 2020, the majority of the studied parameters showed a typical seasonal variation. For example, temperature varied from  $0.0$  °C to  $36.6$  °C (mean  $15.5$  °C), and it remained well above  $0$  °C during winter, except in early 2018 when the temperature was close to  $0$  °C. The highest temperature was almost always recorded in August. Salinity ranged from 13.7 to 32.3 (mean 29.5) and remained steadily high (at  $\sim 30$ ) during winter periods relative to the summertime, when the salinity varied widely following monsoonal precipitation events. The concentrations

of chlorophyll *a* (Chl *a*) were generally below 10 µg/L (mean 5.1 µg/L) during the study period, with a few exceptions when the concentrations were above 50 µg/L, for example, ~100 µg/L in December 2019. In general, Chl *a* showed relatively higher concentrations in the (early) warm seasons than in the cold seasons, depending on temperature and nutrient conditions. Dissolved oxygen (DO) varied from 0.5 to ~15.0 mg/L (15~470 µM) (mean 8.75 mg/L or 272 µM) and showed the opposite trend to the temperature distribution. The DO concentrations were high during warm seasons with high Chl *a* concentrations and were the lowest in the middle of summer with the lowest nutrients and biological production. Occasionally, high DO concentrations coincided with high Chl *a* concentrations and were associated with nutrient input and severe rain events, such as those in August 2018. The pH ranged from 7.32 to 8.68 (mean, 8.06) during our monitoring period. The pH distribution was somewhat similar to the DO distribution, and the summer pH values were lower than those during the winter. The levels of nutrients (total nitrogen and phosphorus, (TN and TP, respectively)) varied widely from the almost depletion concentration to ~2.1 mg/L for both TN and TP, but were mostly ~0.2 and 0.02 mg/L, respectively, during the whole year. However, both TN and TP were elevated occasionally following monsoon or episodic rain events, although the elevations differed every year. Chemical oxygen demand (COD) ranged from ~0.0 to 21.2 mg/L (mean 2.1 mg/L) and did not exhibit clear seasonal or annual trends. The highest COD concentrations were observed in the early cold season of 2017, whereas the lowest concentrations (<0.5 mg/L) were observed in 2020.

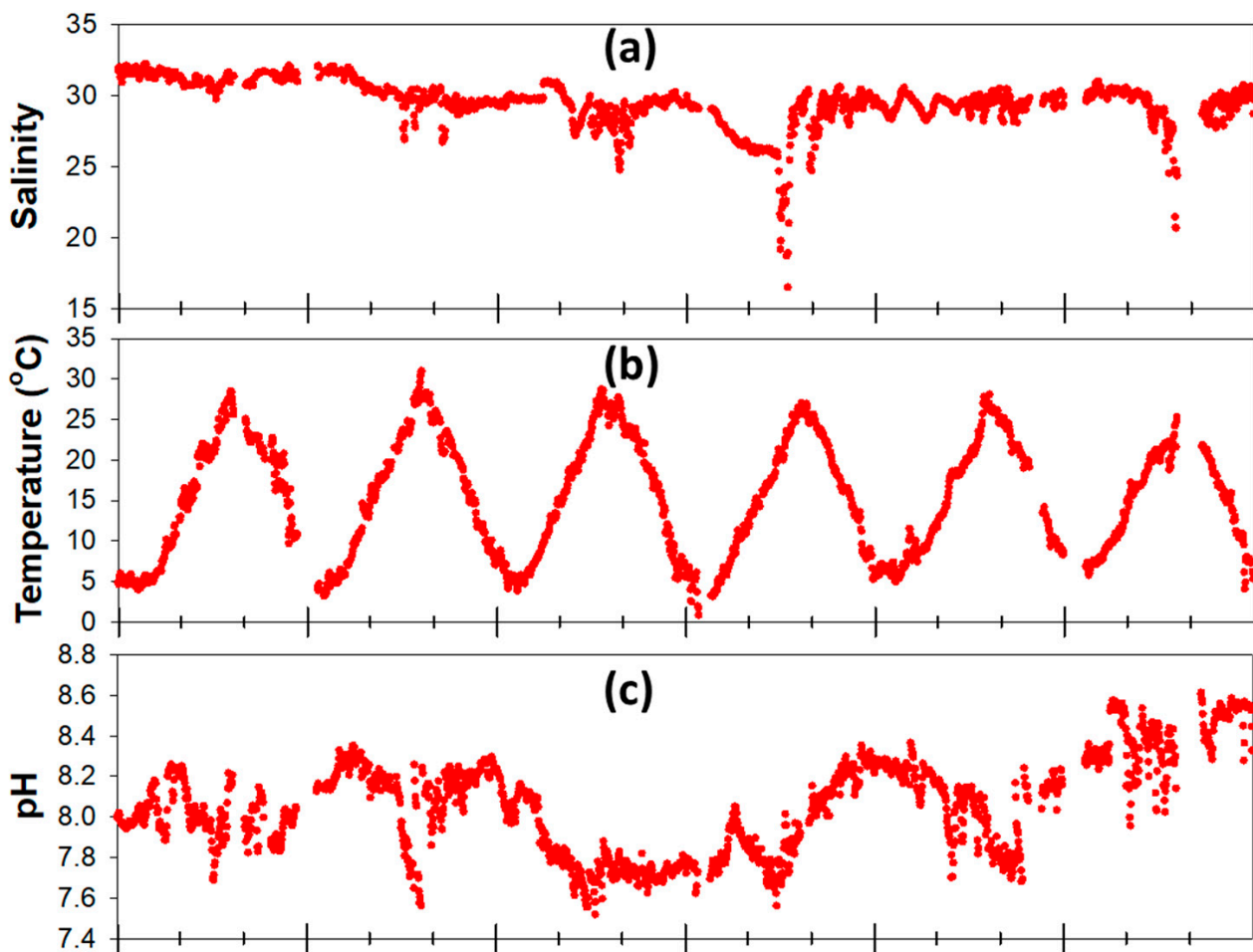
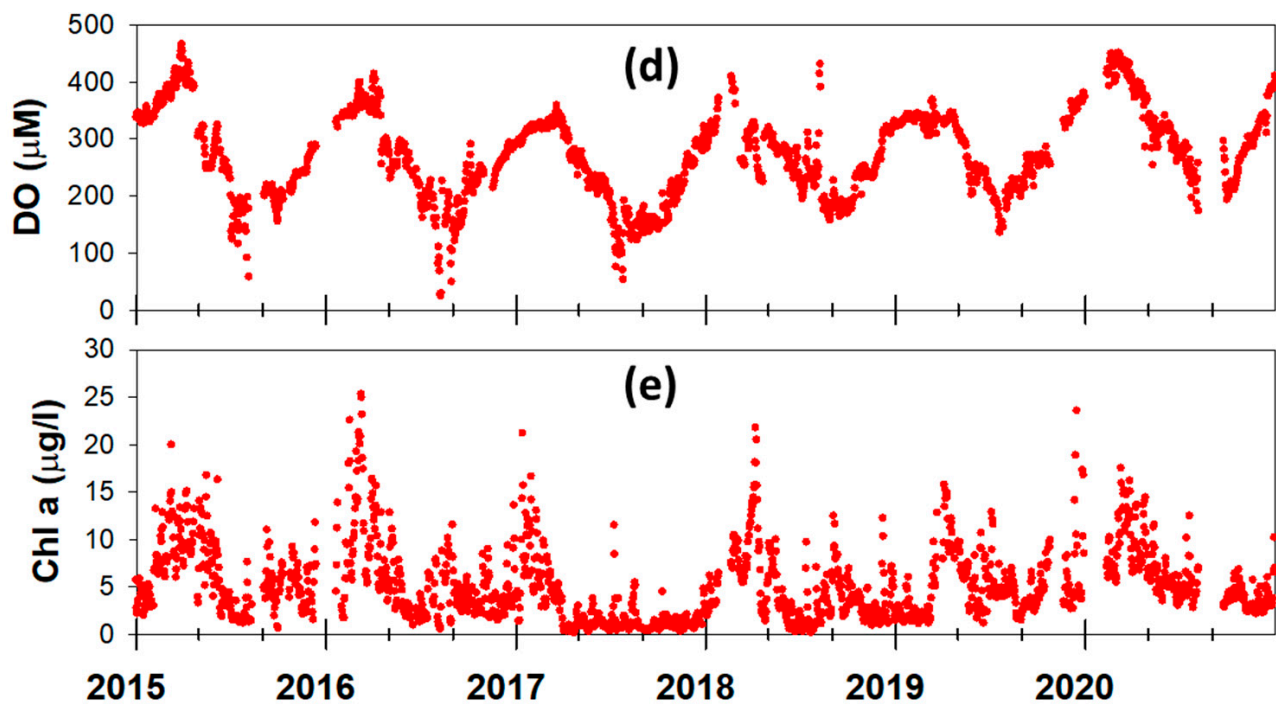
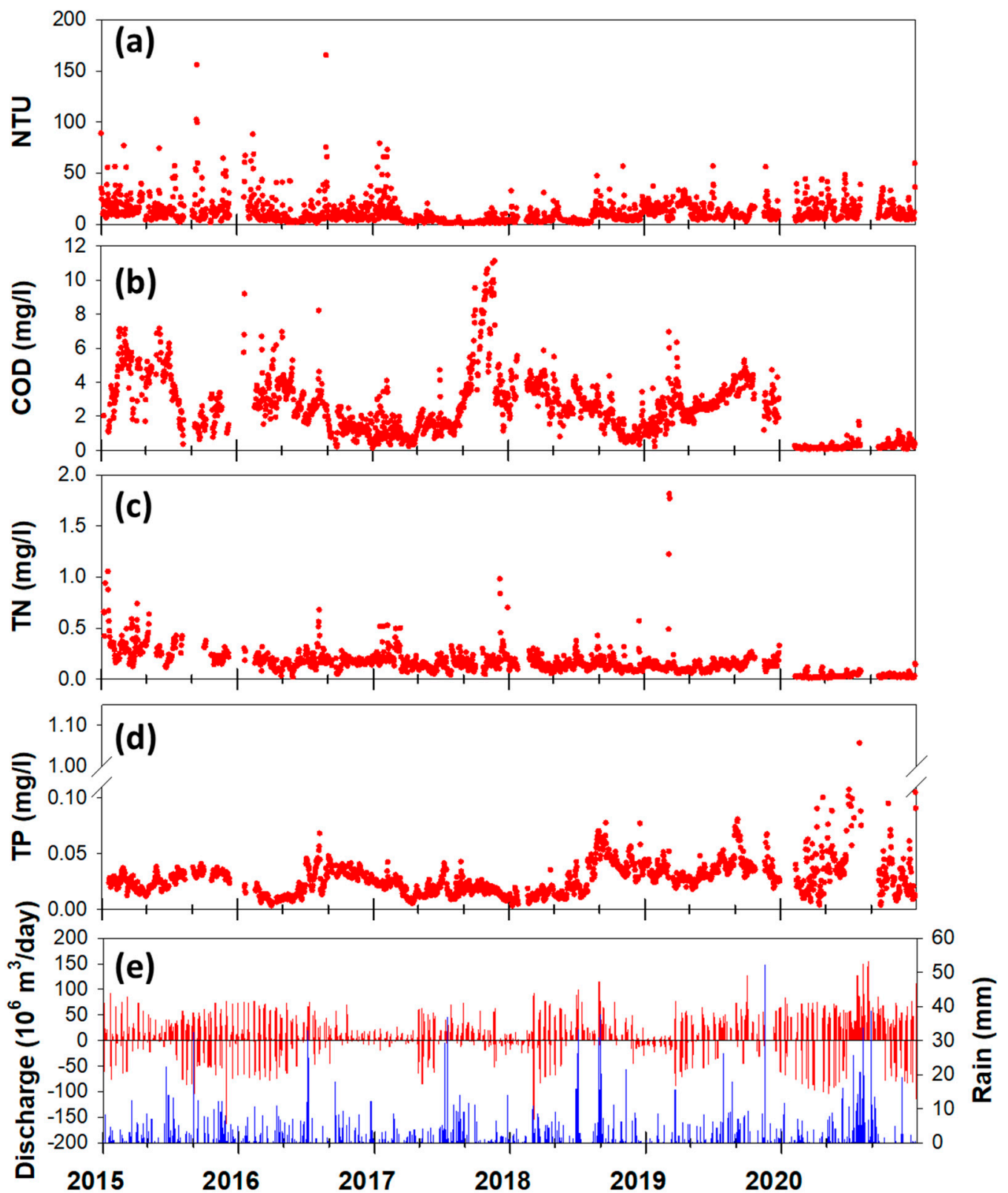


Figure 2. Cont.



**Figure 2.** Variations in the daily averaged parameters: (a) salinity, (b) temperature, (c) pH, (d) dissolved oxygen (DO), and (e) chlorophyll *a* in surface waters during 2015–2020. Note that data, in particular, from early August to late September 2020 when the pH and DO were likely the lowest, are missing (see text for detail).

In general, most variables investigated in this study showed somewhat typical seasonal variations and some episodic variations. For example, temperatures were similar to the reported air temperature around our study region during the last 30 years [19,26] (Kim et al., 2008; Li and Kim, 2019). The surface water DO displayed the opposite trend to that of temperature, suggesting that temperature changes contribute to the surface DO distribution, for example, increasing solubility in cold seasons and degassing in warm seasons. Biological production (i.e., Chl *a* concentration) generally peaked during the early warming season and remained low during the rest of the season but was occasionally elevated upon freshwater input during monsoonal rain events (Figures 2 and 3). Nutrients had no clear seasonal variation throughout the study period (Figure 3). Although we did not monitor water quality in the artificial lake and river waters, TN and TP concentrations were considerably lower in waters outside the sea dike than those in the artificial lake and river waters when compared with observations from previous studies (c.f. [20,21,31]). This nutrient distribution suggests that nutrients were removed in the artificial lake where watershed water could be reserved for a while, and then this low-nutrient lake water was introduced to the open coastal area. However, note that, on some occasions, the lake water discharge likely influenced the TN and TP, particularly during monsoonal rain events when water from the watershed was rapidly introduced to the open coastal water without remaining in the lake. For example, in July 2016 and September 2018, when severe rainfall events and sluice gate opening occurred, both TN and TP were elevated (Figure 3).



**Figure 3.** Variations in daily averaged parameters: (a) turbidity (expressed here in nephelometric turbidity unit; NTU), (b) chemical oxygen demand (COD), (c) total nitrogen (TN), (d) total phosphorus (TP), and (e) water flow (red bar: sluice gate open, blue bar: rainfall at Gunsan metrological site) during 2015–2020.

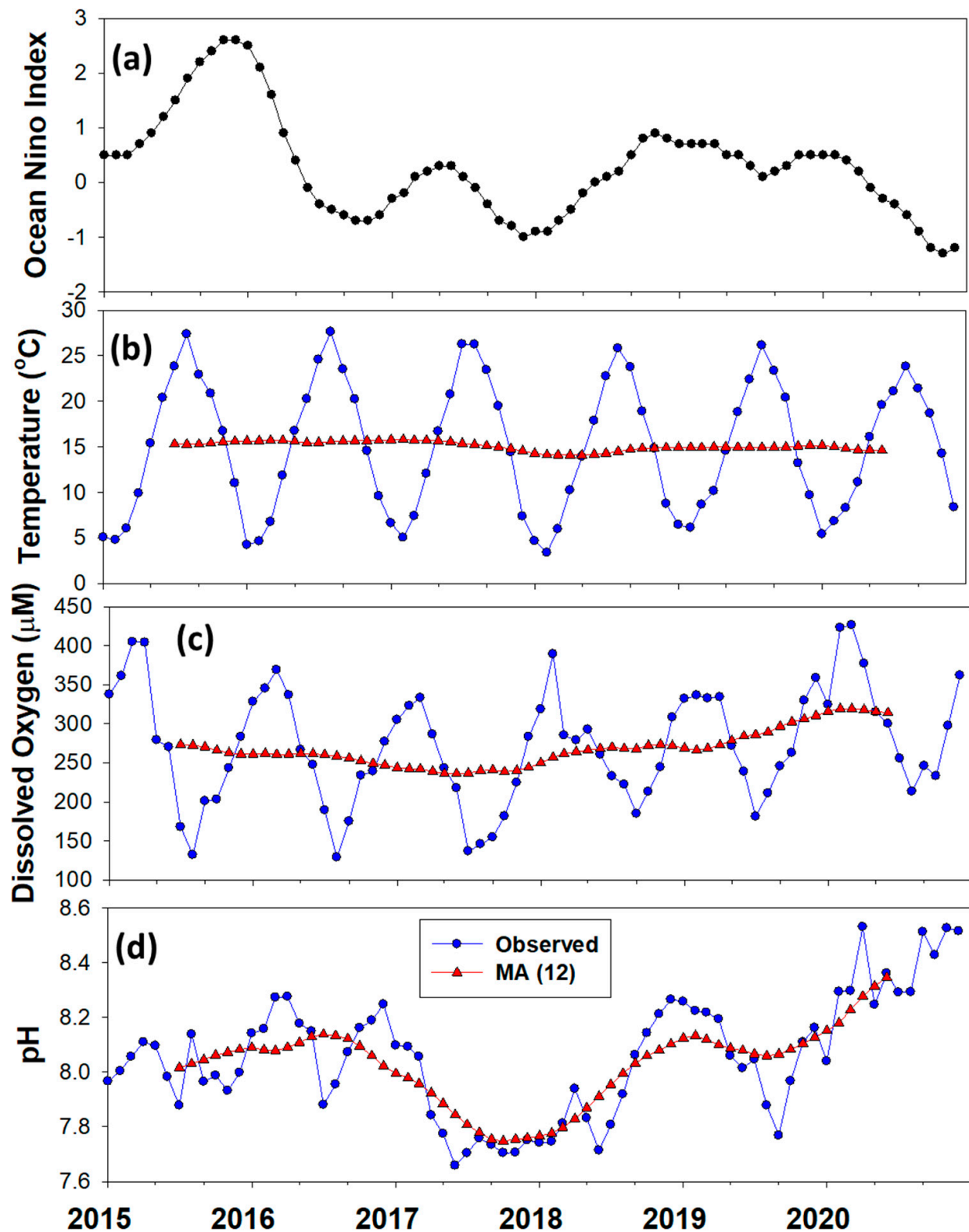


**Figure 4.** Seasonal trends in the monthly averaged variables. (a) Ocean Nino Index in the northwest Pacific Ocean, (b) temperature, (c) dissolved oxygen, and (d) pH. A moving average of 12 months (MA(12)) was applied to investigate the interannual trend (Supplementary Figure S7 presents the other variables). Higher average pH values relative to expected values resulted from the low number of data points for the period of early August to late September 2020.

Annual trends were also investigated using monthly averaged datasets and time-series statistics because some water quality variables could have a long-term trend following pollution control efforts or, potentially, climatological changes [32,33]. Figure 4 (and Supplementary Figure S7) shows the results of the time-series forecasting. Most of the water quality variables in this study did not show clear interannual trends but were seemingly stabilized, probably because of the narrow time window (or small dataset) used to analyze the changes (Figure 4). A noticeable increasing trend was observed for pH, particularly between 2018 and 2020 (Figure 4). Although unclear, this increase in pH may be related to the input of freshwater (or reservoir water) and/or an increase in the primary production (particularly during the late 2019–early 2020 season), which could elevate pH due to high total alkalinity and carbon consumption, respectively [34]. Different long-term trends were observed between the monthly averaged TN and TP. Since mid-2018, TN has shown a decreasing trend, while TP has increased (Supplementary Figure S7). This observation is probably associated with the regulation of fertilizer usage, particularly for nitrogen, as well as the potential inputs of untreated domestic sewage water containing phosphorus [35]. The data for other parameters in this study were scattered without clear trends (Supplementary Figure S7).

### 3.2. Statistical Findings

Basic information on the variables in this study is shown in Supplementary Tables S1–S4. The suitability of PCA was tested, and the Kaiser–Meyer–Olkin index was 0.634 ( $p < 0.0001$ ), indicating that PCA could be useful in determining the variances by reducing the variable dimension. Through PCA, the original nine variables were reduced to three new principal components based on the loading values (eigenvalue  $> 1$ ) and rotations using the varimax with Kaiser normalization (Supplementary Figure S8). These three components explained 65% (32%, 19%, and 14%, for components 1, 2, and 3, respectively) of the total variance in this system (Figure 5a). The first primary component had strong positive loadings on salinity and DO, and a negative loading on temperature, which likely represents natural components (or climate processes). The second component included COD and TN as a positive loading and pH as a negative loading, which seemed to be pollution-related components. Simeonov et al. [27] and Zhou et al. [36] treated COD and nutrients (organic nitrogen and nitrate) as pollutants derived from domestic wastewater. Thus, our study site may have been under the influence of anthropogenic sources to some degree. The third component included suspended solids (i.e., NTU), TP, and Chl *a*, all of which had a positive loading. The TP concentration in this system was considerably lower than that in river water fed into an artificial lake (cf. [21,37]), suggesting that most of the riverine TP was removed in the artificial lake. Therefore, the third component is not likely to represent anthropogenic components but natural processes, such as bottom water resuspension.

Based on hierarchical CA, the water quality parameters can be classified into three clusters depending on the average linkage level: group #1 (pH, DO, Chl *a*, salinity, and NTU); group #2 (COD and TN); and group #3 (temp and TP) (Figure 5b). In cluster 1, DO and pH were the closest link and were clustered with Chl *a*, suggesting that the DO and pH changes in this system were largely influenced by primary production as well as freshwater inputs. The second cluster included COD and TN, which were the same as the second components in the PCA, and this group indicated pollutant inputs. Temperature and TP could be co-varied but were very weakly related. Both statistical analyses indicate that water quality outside the sea dike may be influenced by pollutants to some degree.

Previous studies have commonly found that anthropogenic pollutant inputs are the primary component affecting coastal water quality. Monica and Choi [20] conducted PCA on data from the Dongjin and Mangyeong Rivers and reported that biological oxygen demand (BOD), COD, suspended solids, TN, and TP were the primary components. They described the first component as anthropogenic chemical inputs related to untreated sewage and agricultural runoff [37]. Similarly, Zhou et al. [36] investigated bay waters along the

Hong Kong coast and reported that BOD, nitrate, and total Kjeldahl nitrogen were the primary components representing organic pollution. In northern Greek coastal waters, Simeonov et al. [27] found that COD, BOD, TON, and TP were the first components, reflecting municipal and industrial effluents. Interestingly, natural (or climate) processes were the primary component in our study, which differs from the results of previous studies. This difference in the observed primary component makes sense in that without artificial lakes or reservoirs, polluted water can be directly introduced to open coastal regions. In contrast, in the case of artificial lakes, after a relatively long water residence time in the reservoir, anthropogenic chemicals are removed prior to the release of lake water into an open coastal system. However, we note that the second component (PCA #2) in this study was related to pollutant inputs with positive loadings of COD and TN. Thus, our study site was still under the influence of domestic sewage and/or agricultural runoff, similar to a previous observation of land-derived heavy metals outside the sea dike [17].

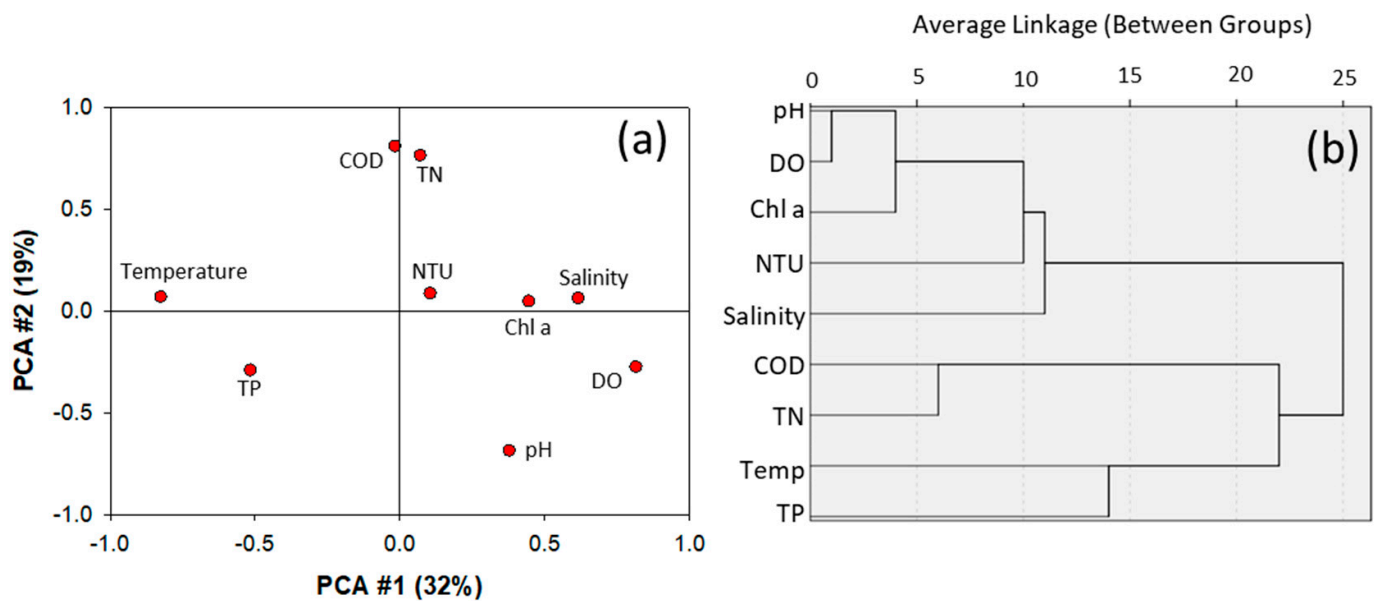


**Figure 5.** Results of statistical analysis: (a) rotated component matrix in principal component and (b) cluster analyses. The rotated component matrix generated by rotation converged in five iterations.

### 3.3. Surface DO Distribution

DO distribution was perhaps the most interesting result of this study. In general, DO concentrations during cold periods were much greater than oxygen saturation. In some cold periods, the DO concentrations were recorded up to ~15.0 mg/L at a salinity of 31.6 and 7.8 °C of water temperature (30 March 2015; 158% supersaturation of DO). This hyperoxic condition is commonly observed in areas with high nutrient supply [38], as well as in the semi-enclosed bays, which are typical along the Korean coast [12,13,39].

DO supersaturation was commonly observed during cold periods (November–April), with peak concentrations in March and April when Chl *a* concentrations peaked (Figures 2 and 3). Although we did not observe a good correlation between DO and Chl *a* in our dataset (Supplementary Figure S9), the increase in temperature during the winter–spring transition is often known to be the primary factor for the depletion of biological nutrients in spring [40,41]. Indeed, nutrient (TN and TP) concentrations were relatively higher in cold periods than in warm periods (Figure 3). Thus, the DO supersaturation in March and April was likely due to DO addition by the primary producers via photosynthesis under the optimal conditions of nutrients and temperature.

While the cold periods showed an intensive DO production and surface supersaturation, DO was severely depleted during some warm periods, decreasing DO saturation to 20% (Supplementary Figure S11). During the warm periods, the primary production

was lower than that in the cold periods, suggesting that the photosynthetic input of DO would be lower and/or DO consumption may be greater in summer relative to that in the cold periods (Supplementary Figure S10). An increase in temperature can decrease DO solubility and lead to degassing. In fact, we found a clear negative correlation between DO and temperature (Supplementary Figure S9), which is commonly observed in other coastal systems (e.g., coastal water in Hong Kong, [36]). However, the degree of DO depletion in this study was far beyond the temperature-salinity adjusted DO saturation (Supplementary Figure S11), and thus, processes other than temperature-induced O<sub>2</sub> degassing must contribute to surface DO depletion. Possible explanations for the low surface DO include the inputs of low oxygen waters from the artificial lake (if DO is depleted), inputs from groundwater [42] and other water bodies that are severely depleted in DO [11], and/or diel-cycling of respiration associated with low DO water at night [13,43]. Unfortunately, we did not collect water samples from the artificial lake (i.e., Saemageum reservoir) or groundwater, and thus, it could not be clearly distinguished whether the low-DO water originated from the lake or groundwater. However, when compared with the results of previous studies on the artificial lake, the water quality outside the sea dike (our dataset) was considerably different (Supplementary Table S5). For example, Kwak et al. [44] surveyed water quality in the artificial lake along the two river pathways and observed very low DO waters (1.8–5 mg/L; 56–156 μM) near the sluice gate, with concentrations similar to those in our study. However, the concentrations of the other parameters (e.g., pH, COD, and TP) in the artificial lake waters were significantly different from those in the water outside the sea dike (Supplementary Table S5). We note that the previous artificial lake surveys were conducted during different seasons, and samples were collected at different depths; thus, a direct comparison between the two systems may not clearly indicate that the two waters were completely different. In addition to the different water qualities inside and outside the sea dike, there was no sluice gate opening or salinity change when the maximum DO depletion occurred (Figure 2), suggesting that the lake waters and fresh groundwaters may have had a minimal influence on surface DO depletion.

The remaining, and perhaps the most likely explanation, could be diel-cycling (or convection) at night and the input of bottom water associated with heterotrophic respiration. Most DO-depleted waters were observed at night (or early in the morning), and in some warm periods, the low DO (less than DO saturation) on the surface persisted even during the daytime (Supplementary Figure S12). This nighttime DO depletion has been commonly observed in many other shallow systems, such as lagoons and bays in Delaware, USA [43], Waquoit Bay in Massachusetts, USA [45], and shallow inner Jinhae Bay in Korea [13], and it occurs mostly due to biological respiration. This phenomenon could last for minutes to several hours [13,43], meaning that respiration-derived low DO can be overcome by daytime DO production. However, in some warm periods, low DO persisted over a day or even weeks (Supplementary Figures S1–S6). The persistence of low DO for a day or even longer suggests that the surface water could have received low-DO water from elsewhere.

The introduction of DO-depleted bottom water (or water from elsewhere) could also contribute to surface DO depletion. Joungh and Shiller [11] found that low-DO surface water in shallow areas of the Louisiana Shelf was caused by an episodic low-DO bottom water introduction associated with wind changes. Because there was no vertical profiling of DO at this monitoring station, we could not determine whether DO in the bottom water had actually been depleted. Most of the southwestern coast of Korea, including our sample collection site, is a tidal mudflat where, typically, the sedimentary oxygen consumption is much higher than that in the water column [46]. Accounting for the large organic matter supply from the in situ production and transport from the lake, the sediments and overlying bottom waters in our study site could easily enter and sustain low oxygen conditions during the summer periods. In addition, the water sample was collected at ~1 m from the surface in a total water depth of 3 m, and thus, bottom water resuspension can be susceptible to wind changes and tidal fluctuations [24,25,47]. Therefore, the surface DO depletion in this

study may be a combination of biological activities in the water column and sediments as well as vertical mixing.

It is currently unclear if the low DO surface water can be attributed to the sea dike construction. However, changes in current direction and speed occurred after the construction of the sea dike [19]. For example, Park et al. [25] and Choi et al. [47] reported a greater reduction in the tidal phase and flow after sea dike construction in approximately the same region as this study site. This dike construction also has a profound impact on water column phytoplankton communities [31], benthic flora [48], and anthropogenic contaminants [49]. Thus, the low oxygen occurrence in this system may be associated with sea dike construction. Nevertheless, as coastal eutrophication extends in size and duration [15,16], this low surface oxygen could also worsen, leading to changes in other chemical properties of water, such as CO<sub>2</sub> elevation and pH decrease [9,50].

### 3.4. pH Changes and Implications of DO Depletion

The interannual variation in pH was generally identical to that in DO (Supplementary Figure S11). However, during some periods, the pH distributions were decoupled from DO variation. For example, in the late 2017 and early 2018 seasons, pH hovered at values of approximately 7.7 for about 5 months, whereas the DO increased. In other words, the pH values in late 2017 were very low compared with those in the other years. During that period, we observed elevated COD concentrations, which was unusual considering that all the other parameters did not show any abnormal variations (Supplementary Figure S3). Although COD is defined as the oxygen concentration required to oxidize all (but mostly labile) organic material into CO<sub>2</sub> and water through chemical oxidation, it also comprises reduced chemical species (e.g., Fe, Mn, and sulfides), all of which reduce DO and pH during reactions in the water column, and can originate from benthic inputs and/or groundwater discharge [51]. Thus, although it is still unclear, the persistence of low pH together with the high COD in late 2017 was likely related to the degradation of COD and the reaction of reduced species, which were accompanied by episodic inputs of local contaminants and/or bottom water to the surface layer. In late 2020, pH showed an increasing trend with values of up to 8.5 (Figure 4). In other words, the pH did not decrease relative to that in the other years. We note that pH data were not collected for over a month from early August to late September 2020, and thus, only a few data points with relatively high values were included in the daily and monthly averages. Typically, the pH was the lowest during this period in the other years when the lowest DO occurred. Nonetheless, considering the interannual variation, the pH in 2020 was slightly higher than that in the other years (Figures 2 and 4). During the mid/late-2020 season, we observed large amounts of freshwater inputs following unusually long monsoonal precipitation events compared with those in the other years (Figure 3). In general, freshwater has a low buffering capacity; thus, the pH could have decreased [34]. However, at the same time, because of the large amount of nutrient input from the watersheds (e.g., TP, Figure 3), the biological production would be high, thereby increasing pH. For example, after freshwater input in Laajahti Bay, Finland, the pH increased from 7.6 to 8.8 [34]. In our study area, especially during 2020, though no data collection over a month in the summer of 2020 limited our understanding, the elevated pH was probably due to an increase in biological production induced by freshwater inputs (Supplementary Figure S7).

Currently, bottom water hypoxia is globally widespread, and the areas and durations of bottom water hypoxia are expected to be greater in the near future [15]. However, biogeochemical changes associated with bottom water hypoxia are not fully understood. When the water column DO is depleted through biological activity, carbon dioxide (CO<sub>2</sub>) can be produced, and subsequently, the pH decreases [9,50]. Therefore, pH is often negatively correlated with DO [9], which was also observed in this study (Supplementary Figure S9). The pH changes caused by DO depletion can be estimated using apparent oxygen utilization (AOU), the Redfield ratio, and total alkalinity [50,52].

When DO is available, the DO consumption (or respiration) process occurs in a manner opposite to that of photosynthesis, that is  $(\text{CH}_2\text{O})_{106}(\text{NH}_3)_{16}\text{H}_3\text{PO}_4 + 138\text{O}_2 \rightarrow 106\text{CO}_2 + 16\text{HNO}_3 + \text{H}_3\text{PO}_4 + 122\text{H}_2\text{O}$  [53]. Based on previous studies (e.g., [9,50,52,54]), the potential changes in pH can be estimated based on the AOU and could be associated with  $\text{CO}_2$  input. Approximation of pH changes can be simplified as  $\Delta\text{pH} = -\log([\text{CO}_2]_{\text{final}}/[\text{CO}_2]_{\text{initial}})$  or simple changes in total  $\text{CO}_2$  concentrations (see details in Sunda and Cai, 2012) and can be calculated using a program developed for  $\text{CO}_2$  systems in MS Excel by NOAA (available at: <https://cdiac.ess-dive.lbl.gov>, accessed 5 June 2022). In this estimation, the highest AOU of  $\sim 180 \mu\text{M}$  could lead to a pH decrease of 0.32 under conditions of  $\sim 2002 \mu\text{mol/kg}$  and  $2382 \mu\text{mol/kg}$  of dissolved inorganic carbon (DIC) and total alkalinity concentrations, respectively, as observed near our study site [55]. This pH decrease is very similar to the estimation calculated for Louisiana Shelf waters, where severe bottom water hypoxia has occurred annually during the last few decades [9,16].

When plotting the AOU against pH, there was a significant correlation ( $r = 0.51$ ,  $n = 1837$ ,  $p < 0.0001$ , Supplementary Figure S9d), indicating that the AOU played a critical role in the pH decrease. The initial pH when the AOU did not occur was 8.04, which is in fairly good agreement with the pH in a typical coastal seawater in the Yellow Sea ( $\sim 8.02$ ). [56] Nonetheless, this suggests that with the maximum AOU of  $\sim 180 \mu\text{M}$ , the pH could decrease to as low as  $\sim 7.50$ , which is considerably lower than the estimated value of 7.72 (decreased by 0.32 from 8.04). With the simplest model employed in this study, it is not possible to explain the cause of the extra pH drop; thus, a sophisticated model and actual measurements of carbon species and total alkalinity are necessary. However, the deviation between the modeled and measured pH was also observed in other systems, such as the shallow northern Gulf of Mexico and East China Sea [9], and in the deep ocean, e.g., the East (Japan) Sea [50]. For example, Cai et al. [9] observed an extra 0.05 pH reduction relative to the estimated pH in Louisiana Shelf waters and concluded that the additional pH decrease was probably associated with a reduction in buffering capacity as the DIC increased in seawater following the increase in  $\text{CO}_2$  in the atmosphere [9,50,54]. Interestingly, their extra pH reduction (0.05) was far smaller than the additional pH drop in this study ( $\sim 0.2$ ). Recently, Cai et al. [57] investigated the pH in waters from Chesapeake Bay, US, and observed a decrease in pH from 8.00 to 7.50 in the mixed layer within  $<2$  days. They suggested that the dramatic pH drop in the mixed layer resulted from vertical mixing because the mid-depth water had a pH of 7.35. Moreover, they suggested that the reduced chemical species, such as  $\text{Fe}^{2+}$ ,  $\text{Mn}^{2+}$ ,  $\text{H}_2\text{S}$ , and  $\text{NH}_4^+$ , could also increase acidity during mixing when these reduced species were oxidized. This upward mixing subsequently reduces the total alkalinity or buffer capacity, resulting in more acidic surface water. Typically, deep waters experiencing bottom water hypoxia, particularly under eutrophic conditions in coastal regions as at our study site, contain considerable amounts of these reduced chemical species [11,58]. Thus, the additional drop in pH relative to the estimated value in this study is probably due to the introduction of other waters from the bottom or other places, such as groundwater, with different chemical properties or, at least, different pH, thereby causing severe ocean acidification. Overall, with the increase in the area and duration of coastal eutrophication and low oxygen water and more  $\text{CO}_2$  input to the ocean from the atmosphere, our results and those of previous studies suggest that coastal environments could have more rapid change and acidification than expected.

#### 4. Conclusions

We monitored the water quality variables in surface waters outside a sea dike where studies are seldom conducted compared with studies of artificial lakes created by sea dikes (or artificial construction). The study was conducted in the Saemanguem area, Korea, where the world's longest sea dike was constructed for land reclamation. Using six years of high-frequency monitoring data and statistical analysis, we found that the water quality at our study site was profoundly influenced by natural processes and some degree of anthropogenic pollutant input. We observed severe surface DO depletion, particularly

during warm periods, and the depletion was as low as 80% of the DO saturation. This DO depletion was likely related to the diel-cycling of respiration production via biological activities. However, on some occasions, DO depletion persisted for much longer than a day, suggesting net respiration and/or a supply of DO-depleted water into the surface layer. In addition, DO was positively correlated with pH, indicating that low DO caused a reduction in the pH. The observed pH was lower than that estimated using a simple DO-pH model. Although an improved model is necessary to estimate the pH decrease from DO depletion, this decrease may be due to the reduction in buffer capacity associated with the atmospheric CO<sub>2</sub> increase and/or in situ generation of CO<sub>2</sub> as well as the introduction of reduced species, particularly in coastal regions.

In the context of global land reclamation efforts involving the construction of sea dikes, our study highlights important findings. Our research reveals that water outside the sea dike can still be affected by pollutants to some degree. Additionally, the construction of such artificial structures can trigger unprecedented environmental events, such as hypoxia, by altering current speed and direction. Considering the expanding areas and durations of coastal eutrophication, the occurrence of low-oxygen water, and the increasing input of CO<sub>2</sub> to the ocean from the atmosphere, our findings, along with previous studies, suggest that coastal environments could undergo rapid changes and acidification beyond initial expectations.

**Supplementary Materials:** The following supporting information can be downloaded at: <https://www.mdpi.com/article/10.3390/jmse11061247/s1>. Figure S1. Temporal variations of water quality parameters in 2015 (original data set). Figure S2. Temporal variations of water quality parameters in 2016. (original data set). Figure S3. Temporal variations of water quality parameters in 2017. (original data set). Figure S4. Temporal variations of water quality parameters in 2018. (original data). Figure S5. Temporal variations of water quality parameters in 2019. (original data). Figure S6. Temporal variations of water quality parameters in 2020. (original data). Figure S7. Variations of monthly averaged parameters and interannual trend using moving average of 12 months (MA(12)). Figure S8. Scree plot of the principal component analysis. Three components were identified by the eigenvalue of > 1. Figure S9. Property–property plots of the variables. (a) Temperature with dissolved oxygen ( $Y = -8.6607x + 403.97$ ,  $n = 1854$ ,  $r = 0.82$ ,  $p < 0.0001$ ), (b) chlorophyll a and dissolved oxygen ( $Y = 9.21x + 226.29$ ,  $n = 1854$ ,  $r = 0.48$ ,  $p < 0.0001$ ), (c) Dissolved oxygen with pH ( $Y = 0.0015x + 7.636$ ,  $r = 0.48$ ,  $n = 1837$ ,  $p < 0.0001$ ), and (d) apparent oxygen utilization (AOU) with pH ( $Y = -0.0024x + 8.039$ ,  $r = 0.52$ ,  $n = 1837$ ,  $p < 0.0001$ ). AOU was determined by subtracting the measured concentration from the saturated concentration. Figure S10. Chlorophyll a and dissolved oxygen (DO) distributions in warm (May–October) and cold (November to April) periods. Monthly averaged. Figure S11. Seasonal variations in the daily averaged parameters: (a) dissolved oxygen and saturation concentrations and (b) dissolved oxygen and pH during 2015–2020. Figure S12. Hourly evolution of DO depletion. The DO depletion was determined by the differences between saturated and measured DO concentrations. Thus, negative values represent a supersaturation of DO. Warm period includes from May to October, while cold period includes November to April. Table S1. Descriptive statistics of data. Table S2. Multivariate coefficients of parameters monitored in this study. Temp.: temperature, DO: dissolved oxygen, NTU: Nephelometric Turbidity Unit, Chl a; chlorophyll a, COD: chemical oxygen demand, TN: total nitrogen, and TP: total phosphorus. Table S3. Scores of principal components for each variable. Table S4. Component Score Coefficient Matrix. Table S5. Comparison of water quality parameters between out- and inside of sea-dyke. (Data from a: This study, b: Kim and Kim, 2002, c: Choi et al., 2013, and d: Kwak et al., 2017). Reference [59] is cited in the Supplementary Materials.

**Author Contributions:** Y.-W.L. and D.K. contributed to the data acquisition. D.J. processed the data. Y.-W.L., D.K., Y.H.O., S.H.L. and D.J. interpreted the biogeochemical data. D.J. wrote the first draft of the manuscript. All authors have read and agreed to the published version of the manuscript.

**Funding:** This work was supported by a Pusan National University Research Grant (202207940001) and a National Research Foundation of Korea (NRF) grant funded by the Korean Government (MSIT) (No. 202215000001) for D.J. Research support for SHL was provided by the Korea Institute of Marine Science and Technology Promotion (KIMST) funded by the Ministry of Oceans and Fisheries (RS-2023-00238264, Development of risk managing technology tackling ocean and fisheries crisis around Korean Peninsula by Kuroshio Current).

**Informed Consent Statement:** Not applicable.

**Data Availability Statement:** The datasets analyzed in this study can be found in the national marine environmental measuring network program. The data are available at [www.meis.go.kr](http://www.meis.go.kr), accessed on 5 June 2022.

**Conflicts of Interest:** The authors declare that the research was conducted in the absence of any commercial or financial relationships that could be construed as a potential conflict of interest.

## References

1. Lotze, H.K.; Lenihan, H.S.; Bourque, B.J.; Bradbury, R.H.; Cooke, R.G.; Kay, M.C.; Kidwell, S.M.; Kirby, M.X.; Peterson, C.H.; Jackson, J.B.C. Depletion, Degradation, and Recovery Potential of Estuaries and Coastal Seas. *Science* **2006**, *312*, 1806–1809. [[CrossRef](#)] [[PubMed](#)]
2. Lohrenz, S.; Fahnenstiel, G.; Redalje, D.; Lang, G.; Chen, X.; Dagg, M. Variations in primary production of northern Gulf of Mexico continental shelf waters linked to nutrient inputs from the Mississippi River. *Mar. Ecol. Prog. Ser.* **1997**, *155*, 45–54. [[CrossRef](#)]
3. Michalak, A.M. Study role of climate change in extreme threats to water quality. *Nature* **2016**, *535*, 349–350. [[CrossRef](#)]
4. Wu, J.; Rong, S.; Wang, M.; Lu, R.; Liu, J. Environmental Quality and Ecological Risk Assessment of Heavy Metals in the Zhuhai Coast, China. *Front. Mar. Sci.* **2022**, *9*, 713. [[CrossRef](#)]
5. Lee, J.S.; Kim, K.H.; Shim, J.; Han, J.H.; Choi, Y.H.; Khang, B.J. Massive sedimentation of fine sediment with organic matter and enhanced benthic–pelagic coupling by an artificial dyke in semi-enclosed Chonsu Bay, Korea. *Mar. Pollut. Bull.* **2012**, *64*, 153–163. [[CrossRef](#)] [[PubMed](#)]
6. Perkins, M.J.; Ng, T.P.; Dudgeon, D.; Bonebrake, T.C.; Leung, K.M. Conserving intertidal habitats: What is the potential of ecological engineering to mitigate impacts of coastal structures? *Estuar. Coast. Shelf Sci.* **2015**, *167*, 504–515. [[CrossRef](#)]
7. Pioch, S.; Kilfoyle, K.; Levrel, H.; Spieler, R. Green Marine Construction. *J. Coast. Res.* **2011**, *61*, 257–268. [[CrossRef](#)]
8. Karim, M.; Sekine, M.; Higuchi, T.; Imai, T.; Ukita, M. Simulation of fish behavior and mortality in hypoxic water in an enclosed bay. *Ecol. Model.* **2003**, *159*, 27–42. [[CrossRef](#)]
9. Cai, W.-J.; Hu, X.; Huang, W.-J.; Murrell, M.C.; Lehrter, J.C.; Lohrenz, S.E.; Chou, W.-C.; Zhai, W.; Hollibaugh, J.T.; Wang, Y.; et al. Acidification of subsurface coastal waters enhanced by eutrophication. *Nat. Geosci.* **2011**, *4*, 766–770. [[CrossRef](#)]
10. Yamaguchi, S.; Hayami, Y. Impact of Isahaya dike construction on DO concentration in the Ariake Sea. *J. Oceanogr.* **2018**, *74*, 565–586. [[CrossRef](#)]
11. Joung, D.; Shiller, A.M. Temporal and spatial variations of dissolved and colloidal trace elements in Louisiana Shelf waters. *Mar. Chem.* **2016**, *181*, 25–43. [[CrossRef](#)]
12. Lee, J.; Park, K.-T.; Lim, J.-H.; Yoon, J.-E.; Kim, I.-N. Hypoxia in Korean Coastal Waters: A Case Study of the Natural Jinhae Bay and Artificial Shihwa Bay. *Front. Mar. Sci.* **2018**, *5*, 70. [[CrossRef](#)]
13. Lee, Y.-W.; Park, M.-O.; Kim, S.-G.; Kim, S.S.; Khang, B.; Choi, J.; Lee, D.; Lee, S.H. Major controlling factors affecting spatiotemporal variation in the dissolved oxygen concentration in the eutrophic Masan Bay of Korea. *Reg. Stud. Mar. Sci.* **2021**, *46*, 101908. [[CrossRef](#)]
14. Kim, Y.-S.; Lee, Y.-H.; Kwon, J.-N.; Choi, H.-G. The effect of low oxygen conditions on biogeochemical cycling of nutrients in a shallow seasonally stratified bay in southeast Korea (Jinhae Bay). *Mar. Pollut. Bull.* **2015**, *95*, 333–341. [[CrossRef](#)]
15. Breitburg, D.; Levin, L.A.; Oschlies, A.; Grégoire, M.; Chavez, F.P.; Conley, D.J.; Garçon, V.; Gilbert, D.; Gutiérrez, D.; Isensee, K.; et al. Declining oxygen in the global ocean and coastal waters. *Science* **2018**, *359*, eaam7240. [[CrossRef](#)] [[PubMed](#)]
16. Rabalais, N.N.; Turner, R.E. Gulf of Mexico Hypoxia: Past, Present, and Future. *Limnol. Oceanogr. Bull.* **2019**, *28*, 117–124. [[CrossRef](#)]
17. Ra, K.; Kim, J.-K.; Kim, E.-S.; Kim, K.-T.; Lee, J.-M.; Lee, H.-J.; Choi, J.-Y.; Won, E.-J. Spatial and temporal variations of trace metals in sediments from the artificial Saemangeum Lake, Korea. *Geochem. J.* **2013**, *47*, 475–487. [[CrossRef](#)]
18. Lie, H.-J.; Cho, C.-H.; Lee, S.; Kim, E.-S.; Koo, B.-J.; Noh, J.-H. Changes in Marine Environment by a Large Coastal Development of the Saemangeum Reclamation Project in Korea. *Ocean Polar Res.* **2008**, *30*, 475–484. [[CrossRef](#)]
19. Kim, C.S.; Lee, S.H.; Son, Y.T.; Kwon, H.K.; Lee, K.H.; Choi, B.H. Variations in subtidal surface currents observed with HF radar in the coastal waters off the Saemangeum areas. *Sea J. Korean Soc. Oceanogr.* **2008**, *13*, 56–66.
20. Monica, N.; Choi, K. Temporal and spatial analysis of water quality in Saemangeum watershed using multivariate statistical techniques. *Paddy Water Environ.* **2015**, *14*, 3–17. [[CrossRef](#)]
21. Monica, N.; Choi, K.-S. Rainfall and Water Quality Characteristics of Saemangeum Area. *Curr. Res. Agric. Life Sci.* **2014**, *32*, 203–209. [[CrossRef](#)]

22. Park, H.; Kim, K.; Kim, Y.-W.; Kim, H. Stakeholder Management in Long-Term Complex Megaconstruction Projects: The Saemangeum Project. *J. Manag. Eng.* **2017**, *33*, 5017002. [CrossRef]
23. Oh, C.-S.; Choi, J.-H. Consideration on Changes of Density Stratification in Saemangeum Reservoir. *J. Korean Soc. Mar. Environ. Energy* **2015**, *18*, 81–93. [CrossRef]
24. Lee, S.; Lie, H.-J.; Song, K.-M.; Cho, C.-H.; Lim, E.-P. Tidal modification and its effect on sluice-gate outflow after completion of the Saemangeum dike, South Korea. *J. Oceanogr.* **2008**, *64*, 763–776. [CrossRef]
25. Park, Y.-G.; Kim, H.-Y.; Hwang, J.H.; Kim, T.; Park, S.; Nam, J.-H.; Seo, Y.-K. Dynamics of dike effects on tidal circulation around Saemangeum, Korea. *Ocean Coast. Manag.* **2014**, *102*, 572–582. [CrossRef]
26. Li, T.; Kim, G. Impacts of Climate Change Scenarios on Non-Point Source Pollution in the Saemangeum Watershed, South Korea. *Water* **2019**, *11*, 1982. [CrossRef]
27. Simeonov, V.; Stratis, J.; Samara, C.; Zachariadis, G.; Voutsas, D.; Anthemidis, A.; Sofoniou, M.; Kouimtzi, T. Assessment of the surface water quality in Northern Greece. *Water Res.* **2003**, *37*, 4119–4124. [CrossRef]
28. Franklin, J.B.; Sathish, T.; Vinithkumar, N.V.; Kirubakaran, R. A novel approach to predict chlorophyll-a in coastal-marine ecosystems using multiple linear regression and principal component scores. *Mar. Pollut. Bull.* **2020**, *152*, 110902. [CrossRef]
29. Kamble, S.R.; Vijay, R. Assessment of water quality using cluster analysis in coastal region of Mumbai, India. *Environ. Monit. Assess.* **2010**, *178*, 321–332. [CrossRef]
30. Gupta, I.; Dhage, S.; Kumar, R. Study of variation in water quality of Mumbai coast through multivariate analysis techniques. *India J. Mar. Sci.* **2009**, *38*, 170–177. Available online: <http://nopr.niscpr.res.in/handle/123456789/4667> (accessed on 5 June 2023).
31. Choi, C.H.; Jung, S.W.; Yun, S.M.; Kim, S.H.; Park, J.G. Changes in Phytoplankton Communities and Environmental Factors in Saemangeum Artificial Lake, South Korea between 2006 and 2009. *Environ. Biol. Res.* **2013**, *31*, 213–224. [CrossRef]
32. Shoda, M.E.; Sprague, L.A.; Murphy, J.C.; Riskin, M.L. Water-quality trends in U.S. rivers, 2002 to 2012: Relations to levels of concern. *Sci. Total Environ.* **2019**, *650*, 2314–2324. [CrossRef]
33. Parmar, K.S.; Bhardwaj, R. Water quality management using statistical analysis and time-series prediction model. *Appl. Water Sci.* **2014**, *4*, 425–434. [CrossRef]
34. Carstensen, J.; Duarte, C.M. Drivers of pH Variability in Coastal Ecosystems. *Environ. Sci. Technol.* **2019**, *53*, 4020–4029. [CrossRef] [PubMed]
35. Cho, M.; Jang, T.; Jang, J.R.; Yoon, C.G. Development of Agricultural Non-Point Source Pollution Reduction Measures in Korea. *Irrig. Drain.* **2016**, *65*, 94–101. [CrossRef]
36. Zhou, F.; Guo, H.; Liu, Y.; Jiang, Y. Chemometrics data analysis of marine water quality and source identification in Southern Hong Kong. *Mar. Pollut. Bull.* **2007**, *54*, 745–756. [CrossRef]
37. Hwang, D.H.; Choi, J.Y.; Yi, S.-M.; Han, D.H.; Jang, S.H. The land use plan and water quality prediction for the Saemangeum reclamation project. *Water Sci. Technol.* **2009**, *59*, 1397–1408. [CrossRef]
38. Qian, W.; Zhang, S.; Tong, C.; Sardans, J.; Peñuelas, J.; Li, X. Long-Term Patterns of Dissolved Oxygen Dynamics in the Pearl River Estuary. *J. Geophys. Res. Biogeosci.* **2022**, *127*, e2022JG006967. [CrossRef]
39. Trowbridge, C.D.; Davenport, J.; Cottrell, D.M.; Harman, L.; Plowman, C.Q.; Little, C.; McAllen, R. Extreme oxygen dynamics in shallow water of a fully marine Irish sea lough. *Reg. Stud. Mar. Sci.* **2017**, *11*, 9–16. [CrossRef]
40. Keller, A.A.; Oviatt, C.A.; Walker, H.A.; Hawk, J.D. Predicted impacts of elevated temperature on the magnitude of the winter-spring phytoplankton bloom in temperate coastal waters: A mesocosm study. *Limnol. Oceanogr.* **1999**, *44*, 344–356. [CrossRef]
41. Van Beusekom, J.E.; Loebel, M.; Martens, P. Distant riverine nutrient supply and local temperature drive the long-term phytoplankton development in a temperate coastal basin. *J. Sea Res.* **2009**, *61*, 26–33. [CrossRef]
42. Sanial, V.; Moore, W.S.; Shiller, A.M. Does a bottom-up mechanism promote hypoxia in the Mississippi Bight? *Mar. Chem.* **2021**, *235*, 104007. [CrossRef]
43. Tyler, R.M.; Brady, D.C.; Targett, T.E. Temporal and Spatial Dynamics of Diel-Cycling Hypoxia in Estuarine Tributaries. *Estuaries Coasts* **2008**, *32*, 123–145. [CrossRef]
44. Kwak, D.-H.; Jeon, Y.-T.; Hur, Y.D. Phosphorus fractionation and release characteristics of sediment in the Saemangeum Reservoir for seasonal change. *Int. J. Sediment Res.* **2018**, *33*, 250–261. [CrossRef]
45. D’Avanzo, C.; Kremer, J.N. Diel Oxygen Dynamics and Anoxic Events in an Eutrophic Estuary of Waquoit Bay, Massachusetts. *Estuaries* **1994**, *17*, 131–139. [CrossRef]
46. Cammen, L. Annual bacterial production in relation to benthic microalgal production and sediment oxygen uptake in an intertidal sandflat and an intertidal mudflat. *Mar. Ecol. Prog. Ser.* **1991**, *71*, 13–25. [CrossRef]
47. Choi, B.; Kim, K.; Lee, H.; Yuk, J. Perturbation of regional ocean tides due to coastal dikes. *Cont. Shelf Res.* **2010**, *30*, 553–563. [CrossRef]
48. Ryu, J.; Nam, J.; Park, J.; Kwon, B.-O.; Lee, J.-H.; Song, S.J.; Hong, S.; Chang, W.K.; Khim, J.S. The Saemangeum tidal flat: Long-term environmental and ecological changes in marine benthic flora and fauna in relation to the embankment. *Ocean Coast. Manag.* **2014**, *102*, 559–571. [CrossRef]
49. Yoon, S.J.; Hong, S.; Kwon, B.-O.; Ryu, J.; Lee, C.-H.; Nam, J.; Khim, J.S. Distributions of persistent organic contaminants in sediments and their potential impact on macrobenthic faunal community of the Geum River Estuary and Saemangeum Coast, Korea. *Chemosphere* **2017**, *173*, 216–226. [CrossRef]

50. Chen, C.-T.A.; Lui, H.-K.; Hsieh, C.-H.; Yanagi, T.; Kosugi, N.; Ishii, M.; Gong, G.C. Deep oceans may acidify faster than anticipated due to global warming. *Nat. Clim. Chang.* **2017**, *7*, 890–894. [[CrossRef](#)]
51. Shanmugam, P.; Neelamani, S.; Ahn, Y.-H.; Philip, L.; Hong, G.-H. Assessment of the levels of coastal marine pollution of Chennai city, Southern India. *Water Resour. Manag.* **2006**, *21*, 1187–1206. [[CrossRef](#)]
52. Park, P.K. The Processes Contributing to The Vertical Distribution of Apparent pH In the Northeastern Pacific Ocean. *J. Oceanol. Soc. Korea* **1968**, *3*, 1–7.
53. Redfield, A.C. The influence of organisms on the composition of seawater. *Sea* **1963**, *2*, 26–77.
54. Sunda, W.G.; Cai, W.-J. Eutrophication Induced CO<sub>2</sub>-Acidification of Subsurface Coastal Waters: Interactive Effects of Temperature, Salinity, and Atmospheric PCO<sub>2</sub>. *Environ. Sci. Technol.* **2012**, *46*, 10651–10659. [[CrossRef](#)] [[PubMed](#)]
55. Hwang, Y.; Lee, T. The Buffer Capacity of the Carbonate System in the Southern Korean Surface Waters in Summer. *J. Korean Soc. Oceanogr.* **2022**, *27*, 17–32. [[CrossRef](#)]
56. Zhai, W.-D.; Zheng, N.; Huo, C.; Xu, Y.; Zhao, H.-D.; Li, Y.-W.; Zang, K.-P.; Wang, J.-Y.; Xu, X.-M. Subsurface pH and carbonate saturation state of aragonite on the Chinese side of the North Yellow Sea: Seasonal variations and controls. *Biogeosciences* **2014**, *11*, 1103–1123. [[CrossRef](#)]
57. Cai, W.-J.; Huang, W.-J.; Luther, G.W.; Pierrot, D.; Li, M.; Testa, J.; Xue, M.; Joesoef, A.; Mann, R.; Brodeur, J.; et al. Redox reactions and weak buffering capacity lead to acidification in the Chesapeake Bay. *Nat. Commun.* **2017**, *8*, 369. [[CrossRef](#)]
58. Oldham, V.E.; Owings, S.M.; Jones, M.R.; Tebo, B.M.; Luther, G.W. Evidence for the presence of strong Mn(III)-binding ligands in the water column of the Chesapeake Bay. *Mar. Chem.* **2015**, *171*, 58–66. [[CrossRef](#)]
59. Kim, J.G.; Kim, Y.S. Application of Ecosystem Model for Eutrophication Control in Coastal Sea of Saemankeum Area -1. Characteristics of Water Quality and Nutrients Released from Sediments-. *Korean J. Fish. Aquat. Sci.* **2002**, *35*, 348–355. [[CrossRef](#)]

**Disclaimer/Publisher’s Note:** The statements, opinions and data contained in all publications are solely those of the individual author(s) and contributor(s) and not of MDPI and/or the editor(s). MDPI and/or the editor(s) disclaim responsibility for any injury to people or property resulting from any ideas, methods, instructions or products referred to in the content.